Ceramics International 48 (2022) 29540–29545

Contents lists available at ScienceDirect

Ceramics International

journal homepage: www.elsevier.com/locate/ceramint

Selective laser sintering of alumina-molybdenum nanocomposites

C. Gómez-Rodríguez [a,b], L.V. García-Quiñonez [c], L.F. Verdeja [b], G.A. Castillo-Rodríguez [d], J.A. Aguilar-Martínez [d], A.E. Mariño-Gámez [d], D. Fernández-González [e,*]

[a] Departamento de Mecánica, Facultad de Ingeniería, Campus Coatzacoalcos, Universidad Veracruzana, Av. Universidad Km 7.5 Col. Santa Isabel, Coatzacoalcos, 6535, Veracruz, Mexico
[b] Departamento de Ciencia de los Materiales e Ingeniería Metalúrgica, Escuela de Minas, Energía y Materiales, Universidad de Oviedo, 33004, Oviedo/Uviéu, Asturias, Spain
[c] CONACYT-Centro de Investigación Científica y de Educación Superior de Ensenada, B.C (CICESE), Parque de Innovación e Investigación, Carretera Aeropuerto, 66612, Apodaca, Mexico
[d] Facultad de Ingeniería Mecánica y Eléctrica, Universidad Autónoma de Nuevo León, Av. Pedro de Alba s/n, 66455, San Nicolás de los Garzas, Mexico
[e] Nanomaterials and Nanotechnology Research Center (CINN-CSIC), Universidad de Oviedo (UO), Principado de Asturias (PA), Avda. de la Vega, 4-6, 33940, El Entrego, Spain

ARTICLE INFO

Keywords:
Selective laser sintering
Molybdenum
Alumina
Refractories
Nanocomposite
Toughness

ABSTRACT

Alumina/molybdenum nanocomposites were obtained from alumina and molybdenum particles. Alumina with different molybdenum contents (0, 1, 2.5, 5, 10 and 20 wt %) was first uniaxially pressed at 100 MPa to obtain green compacts that were later sintered using a carbon dioxide (CO_2) laser. Samples were characterized by X-ray diffraction and Scanning Electron Microscope to evaluate the morphological and microstructural characteristics of the composites. SEM results show that for mixtures with 1, 2.5, 5 and 10 wt % Mo, metallic Mo appears dispersed within the alumina grains (grain boundaries and triple points). Nevertheless, for the mixture with 20 wt % Mo, it also appears in the alumina matrix as Mo in triple points and grain boundaries, although MoO_3 is also identified (as inclusion). The presence of these phases was confirmed by X-ray Diffraction technique. These metallic molybdenum particles distributed in the alumina matrix at triple points and grain boundaries promote the densification of the composite. Metallic molybdenum has also a pinning effect, which drastically affects the microstructural evolution during the sintering, mainly on the grain size of alumina. The best results were observed for the composite Al_2O_3-10 wt % Mo, with an average alumina grain size <10 μm and few pores.

1. Introduction

High alumina bricks are widely used in industrial furnaces due to the great characteristics of high temperature performance, great corrosion and wear resistances, among others. However, fracture toughness is sometimes a problem for certain engineering applications. For that reason, several methods have been proposed to improve the fracture toughness in ceramics, mainly based on the crack deflection, which can be made with fibers or whiskers, nacre-like structure or hard second phases. The incorporation of a second phase, such as metallic particles, to the alumina matrix has been subject of research for many years [1]. This way, Matteazzi and Le Caër synthesized nanometric α-Al_2O_3-M composites, where M was Fe, V, Cr, Mn, Co, Ni, Cu, Zn, Nb, Mo, W, Si and Fe alloys [2], which were sintered by aluminothermic reduction. Waku and co-workers also investigated Al_2O_3–Mo, -Ta, -Nb composites prepared by hot pressing [3]. Other composites Al_2O_3-metal have been proposed to improve the fracture toughness: Al_2O_3–Ni [4–7] and Al_2O_3–W [4,8]. However, molybdenum appears as the metal with the greatest interest to reinforce alumina ceramics when fracture toughness is considered. It has been added in the form of metallic powders, MoO_3 or Mo fibers [9–11]. Nawa and collaborators sintered Al_2O_3–Mo composites by hot pressing under vacuum conditions [12]. Wang and co-authors prepared Al_2O_3–Mo composites by different methods: dissolution of MoO_3 powder in ammonia solution followed by spray-drying or hot-plate drying before hot pressing under hydrogen reductant atmosphere; mechanical mixing and hot pressing [13]. Lada and others prepared Al_2O_3-10 vol % Mo composites by aqueous gel casting method and sintering in argon atmosphere at 1600 °C for 2 h with very slow heating and cooling rates [14]. Broniszewski et al. sintered alumina-molybdenum composites from powders by hot pressing at

* Corresponding author.
E-mail address: d.fernandez@cinn.es (D. Fernández-González).

https://doi.org/10.1016/j.ceramint.2022.08.058
Received 27 April 2022; Received in revised form 1 July 2022; Accepted 6 August 2022
Available online 11 August 2022

1350 °C for 1 h under a pressure of 20 MPa in argon atmosphere [15]. Zygmuntowicz and researchers obtained Al_2O_3–Mo composites by centrifugal slip casting method and sintering at 1400 °C for 2 h under 20 vol % H_2-80 vol % N_2 atmosphere [16]. Several questions arise from the above-mentioned research: the improvement of the fracture toughness resulted from both the second phase (molybdenum) on the composite and the inhibition of the alumina grain growth, and the requirement of long sintering processes under special atmosphere (in general reductant) to avoid the oxidation of the molybdenum (to form molybdenum (VI) oxide (MoO_3)), whose boiling point is at 1155 °C.

On the other hand, selective laser sintering (SLS) is a technique that allows the consolidation of powder layers, sintering layer after layer, to obtain three-dimensional parts with fine finishes and complex shapes, being an efficient, economical, high-precision and fast process. Two different types of lasers are commonly used Nd:YAG and carbon dioxide (CO_2). The type of material that can be studied with each laser mainly depends on both the wavelength that each laser generates (1.64 μm and 10.64 μm, respectively) and the wavelength that each material can absorb. Different materials have been treated using laser as heat source for the selective sintering of metallic, ceramic and polymer powders, or mixes between them [17–20]. Great part of the studies in the sintering using laser have focused on the variables that depend on the laser and have direct influence in the properties of the obtained parts: scanning speed [21], scan spacing [22,23], energy density [24,25], laser scanning strategy [26], layer thickness [22,27], laser power [24], particle size and distribution [28].

There is little research about the selective laser sintering of alumina parts. Part of this research focuses on the preparation of powders for later sintering in furnace [29,30]. Regarding direct sintering of alumina (or alumina with additives) using selective laser sintering, it is possible to report the research of Fayed et al. [31] that employed Nd:YAG laser to sinter alumina parts; Shishkovsjy and collaborators reported alumina-zirconium porous ceramics manufactured by selective laser sintering using Nd-YAG laser [32]; Subramanian and Marcus sintered alumina with aluminum by Nd-YAG selective laser sintering with subsequent treatment in furnace at different temperatures and times to study the effect [33]. Alumina-molybdenum cermet manufactured using selective laser sintering was not yet reported in the literature.

Despite the significant interest of the alumina-metal composites to obtain alumina-base refractories with improved the fracture toughness (and flexural strength), and the potential advantages of laser sintering technique related with the economization of the processing time, this technique has not been already applied to manufacture such composites. This way, considering the high melting points of the considered materials (Al_2O_3, 2072 °C; Mo, 2623 °C), a heating source as the CO_2 laser was employed. Therefore, we present in this manuscript novel research about the utilization of the selective laser sintering to obtain alumina-Mo composites. The influence of the molybdenum content (0, 1, 2.5, 5, 10 and 20 wt %) on the microstructure and morphology of the composite was studied when the green compacts were irradiated with carbon dioxide laser.

2. Experimental

2.1. Raw materials and sample preparation

Powders of aluminum oxide (Al_2O_3, 99.9% purity, J.T. Baker) and molybdenum (Mo, 99.9% trace metals basis, Sigma Aldrich) were used as raw materials. SEM images of the initial powders are reported in Fig. 1. These images indicate that most of the molybdenum initial particles are nanometric while the size of the alumina initial particles is in the range 20–100 μm. Six compositions of Al_2O_3 and Mo samples were prepared with the objective of studying the influence of the molybdenum content on the microstructure of the ceramic-metal composite. The samples were prepared considering the following relation: (100−X) wt. % Al_2O_3 + X wt. % of Mo, where X = 0, 1, 2.5, 5, 10 and 20). Once weighted the starting materials in the above-indicated proportion, raw materials were loaded in an attrition mill with alumina balls (3 mm in diameter) in a ratio of 10 to 1 and using isopropyl alcohol as milling medium. Blending was carried out for 5 h in order to ensure a homogeneous mixture. Powder mixtures were treated at 120 °C for 24 h to remove any traces of alcohol and dry powders were sieved by 180 μm. Powders mixture (1 g) were uniaxially pressed in a metallic mold to obtain cylindrical samples of 7 mm in height and 12 mm in diameter using a pressure of 100 MPa for 2 min. A SEM image of the green

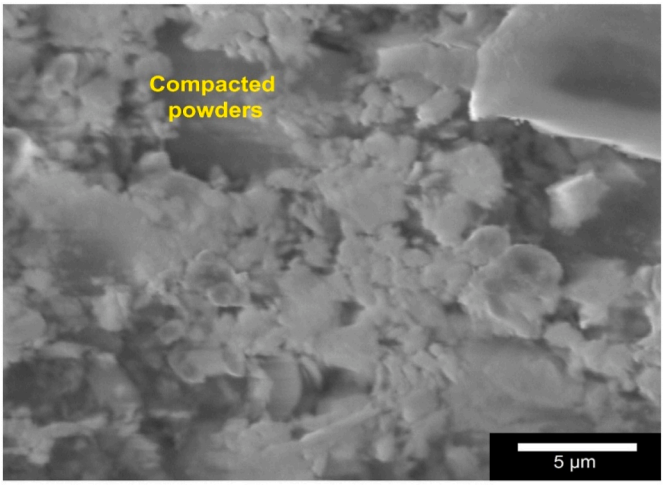

Fig. 2. SEM image of the green compacts. (For interpretation of the references to colour in this figure legend, the reader is referred to the Web version of this article.)

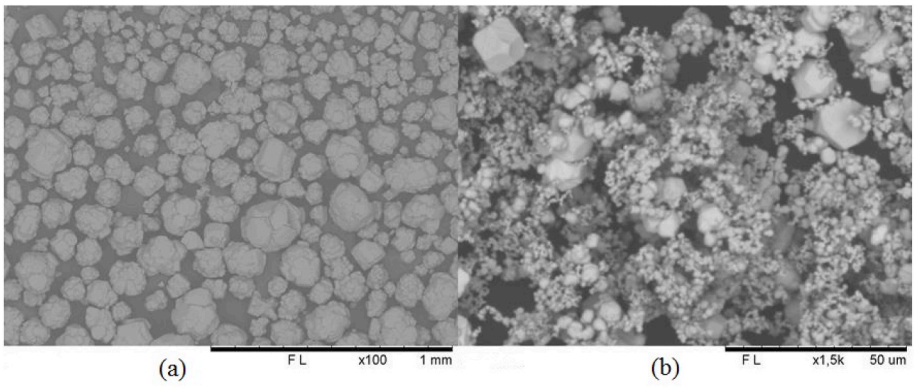

Fig. 1. SEM images of the initial powders of alumina (a) and molybdenum (b).

compacts is reported in Fig. 2 to check the difference with the specimen sintered using laser of CO_2.

2.2. Laser sintering

Green compacts were sintered by means of a CO_2 laser equipment (Coherent, Diamond k-150 model with a wave length $\lambda = 10.64$ μm), where the laser irradiation was perpendicular to the circular surface of the samples. The laser nozzle is fixed in this equipment and the sample was placed on the translation system, which was programmed to move longitudinally, so a parallel radiation was achieved on the diameter of the samples. Subsequently, two more irradiation routes were assigned one next to the other. The sintering resulted on morphological and microstructural changes of the sample.

The following selective laser sintering parameters were considered in this investigation: laser power of 79.5 W, spot diameter of the laser beam of 3 mm and scanning distance of 12 mm. Moreover, the irradiation power density is $Q = 70.29$ W/cm^2 and the translation speed was 1.25 mm/s. There is a distance between the laser nozzle and the surface of the sample of 35 mm. Green compacts are located on the surface of the translation equipment and experiments were carried out at room temperature and under ambient atmosphere.

2.3. Characterization

X-ray diffraction technique was used to identify the crystalline phases at the end of the selective laser sintering process. The equipment where the diffraction patterns were obtained was a PANalytical EMPYREAN diffractometer with a target of metal cobalt (radiation K_α = 1.5406 Å) operated at 40 kV, 40 mA and an X'Celerator detector in Bragg-Brentano geometry. The scans were carried out over a 2θ range from 5° to 120° with a step scan of 0.013° and 25.5 s per step in a continuous mode. Peak fitting was carried out with the commercial software XPowder12.

3. Results

3.1. X-ray diffraction

Results of the X-ray diffraction analyses of laser sintered samples are summarized in Fig. 3. The oxidation of molybdenum has been subject of significant research throughout the years [34,35], because metallic molybdenum exhibits good mechanical properties at high temperatures but the resistance to oxidation is really poor. This way, at temperatures greater than 400 °C oxidizes to form MoO_3, which easily volatilizes

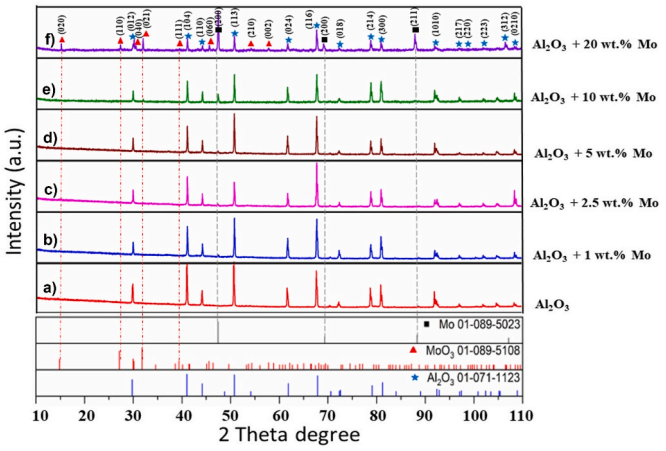

Fig. 3. XRD patterns of: (a) Aluminium oxide (Al_2O_3) sample and (b–f) samples containing 1, 2.5, 5, 10 and 20 wt % of Mo, respectively. At the bottom, the diffraction patterns of Al_2O_3, MoO_3 and Mo are observed.

(1155 °C). This is a problem in the manufacture of composites with molybdenum as this element is lost during their manufacture, as for instance in the case of graphite-molybdenum composites sintered at high temperatures (2600 °C [36]). X-ray diffraction analyses suggest that oxidation of molybdenum for contents <10 wt % is not relevant and peaks correspond to only molybdenum and aluminum oxide, which might be associated to the sintering speed. X-ray diffraction analysis of alumina-20 wt % molybdenum composite indicates the presence of molybdenum (VI) oxide, which as it is later observed in SEM-EDX analyses, tends to agglomerate and the pinning effect of the molybdenum microparticles disappear.

3.2. SEM-EDX

The morphological characterization was performed by Field Emission Scanning Electron Microscopy (FESEM) using a FEI Nova Nano SEM 200, with an acceleration voltage of 10-15 kV in low vacuum mode and an Helix detector; additionally, energy dispersive X-ray microanalysis, EDX (Oxford, model INCA X-Sight) was also carried out for semi-quantitative chemical microanalysis. Images are collected in Fig. 4. It is possible to see that molybdenum clearly appears at grain boundaries and triple points, particularly for the composite Al_2O_3-10 wt % Mo. It is precisely in this sample where few pores are identified in the micrographs, which suggest high densification rates. In other cases, there are empty spaces at triple points and grain boundaries that suggest that the sintering of the composite was not complete. It is also possible to see in these cases that grain has grown during the selective laser sintering process, probably due to the insufficient quantity of molybdenum in some cases (when Mo content is < 10 wt %) and to the significant oxidation of the molybdenum (when Mo content is > 10 wt %). The sample with 10 wt % has the smallest grain size (<10 μm), precisely promoted by the fine molybdenum particles located at triple points and grain boundaries that have a pinning effect. As it was observed in the X-ray diffraction analyses, molybdenum (VI) oxide appears as inclusions in several points of the microstructure for the greatest molybdenum contents (20 wt %). This question is highly relevant for the mechanical properties of the composite as these inclusions appear as stress concentration sites in the composite. In the other cases, metallic molybdenum particles clearly appear at triple points and grain boundaries (see Fig. 4).

3.3. Discussion

The reinforcement of ceramic materials, and in particular alumina ceramics, has always attracted significant interest in an attempt to promote the mechanical properties (as well as the slag corrosion resistance in other cases) by second phases located at triple points and grain boundaries that could divert the crack during its propagation. These second phases also avoid the grain growth and, in this way, a fine grained structure has a significant length of grain boundary, which is beneficial to avoid crack propagation. This manuscript collects a novel research about the application of selective laser sintering to manufacture Al_2O_3–Mo ceramic materials with the aim of studying the microstructure and analyzing how this could have influence on the mechanical properties, in particular on the fracture toughness.

The main problem of the molybdenum is that it easily oxidizes under sintering conditions and this habitually requires sintering the molybdenum-based composites, and Al_2O_3–Mo, under special atmospheres as Ar/H_2 [37], vacuum [12,38], argon [14,15] or H_2/N_2 [16]. In this way, the utilization of fast sintering techniques, as laser, might be useful to minimize the losses of molybdenum as molybdenum (VI) oxide during the sintering process and, at the same time, obtain dense composites. It was possible to see for molybdenum contents <10 wt % that molybdenum (VI) oxide does not appear during the X-ray diffraction analyses (this phase appears in the sample with 20 wt % molybdenum), although this is not indicative of potential minimum losses of this

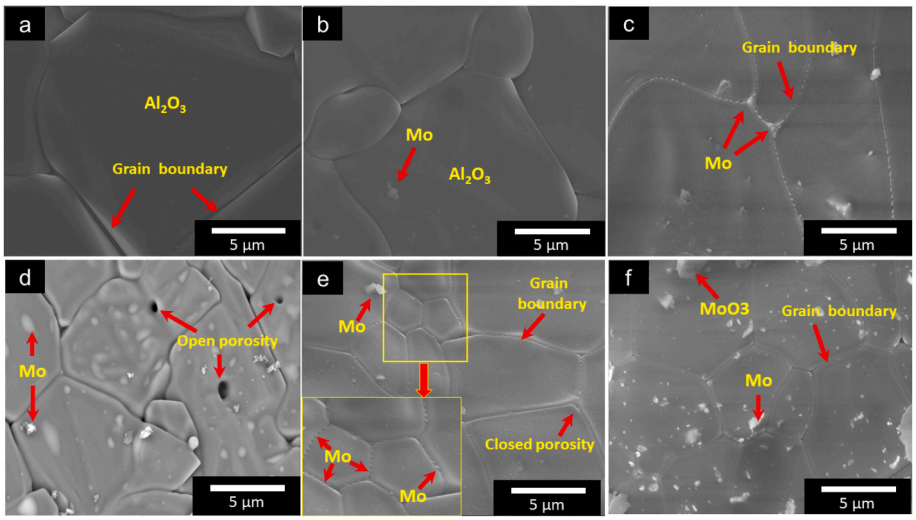

Fig. 4. SEM images of irradiated samples, where: (a) corresponds to Al_2O_3 particles and (b–f) corresponds to 1, 2.5, 5, 10 and 20 wt% of Mo, respectively.

element during the sintering process of the composites with <10 wt % Mo. SEM technique suggests pining effect promoted by the metallic molybdenum and few pores, which indicates that sintering of the Al_2O_3–Mo composite could be achieved without special atmosphere for these contents of molybdenum. This is potentially beneficial because near-net shape sintered samples could be obtained in very short times without using any special atmosphere, which otherwise could complicate the process. Therefore, laser sintering of ceramic materials arises as a technology that could compete with other novel high energy density technologies as solar energy [39–46] or spark plasma sintering [47,48]. This way, competitiveness of ceramic industry could increase because sintered ceramic materials might be obtained in shorter times. Selective laser sintering technique is a good option to sinter ceramics because it is a versatile technique, which is one of the aspects that is being searched by the industry and, particularly by the additive manufacturing industry. The reason is that this technology allows the rapid fabrication of functional parts, in addition to having the ability to process a wide range of materials (polymers, ceramics and metals) [49], although the manufacture of dense alumina ceramics is still to be studied. Therefore, this manuscript could be a starting point to study the obtaining of dense ceramics using laser technology. There is currently a wide variety of manufacturing techniques, but the most attractive and of greatest importance to the industrial sector are, naturally, those that provide high efficiency in production output without neglecting quality standards. Therefore, one of the most cost-effective methods for manufacturing complex 3D parts is the selective laser sintering technique, which has achieved the highest market share growth since 1997 [50].

Based on several studies [51–56], selective laser sintering could provide a number of advantages as the selection of any specific area, sintering at room temperature (with the sintering temperature being reached only in the surface of the beam), sintering of layers of microns in thickness, selection of the area that is to be irradiated, among others as the possibility of operating under two methods of irradiation, punctual or translational, where in this last case, it is possible to adjust the speed of the beam and the direction of irradiation. Moreover, it is possible to process parts of considerable size. Anyway, the greatest interest of this technology arises from the possibility of obtaining microstructures and morphologies of sintered refractories in seconds, which are comparable with those obtained by means of other sintering methods (as the sintering in furnace) that require hours. This could relate with the productivity but also with the savings in manufacturing costs, the reduction in energy consumption, and, therefore, this process could be environmentally friendly and could attract interest of the industry of ceramics in general.

There are two laser sources used for the Selective Laser Sintering of materials which are, continuous wave CO_2 with a wavelength of 10.6 µm, and Nd:YAG laser of wavelength 1.06 µm with pulsed or continuous mode [57]. The use of the laser source for each material is mainly governed by the percentage of energy absorption of each material. In the research presented in this manuscript, laser of CO_2 was chosen because we know that the matrix of the composite (Al_2O_3) has high absorption (96% of wavelength of 10.6 µm with CO_2 laser) with long wavelengths [50]. In the case of metals, as molybdenum, it is known that they absorb shorter wavelengths. This way, a sufficient amount of energy was supplied to induce high local temperature leading the beginning of the solid-state sintering. Thus, when the Al_2O_3 atoms were irradiated, they had sufficient energy to make that the vacancies of the Al_2O_3, which are in the hexagonal structure of the aluminum oxide, were replaced at high temperature by other cations that are inside of the volume of the crystal of the aluminum oxide. Therefore, there is a migration towards the grain boundaries, making the grain boundaries to start to move and grow due to the cationic movement, which takes place in the same direction. This growth associated to the movement of cations is drastically affected by the molybdenum particles, located at triple points and grain boundaries, avoiding the growth of the grains and the movement of the grain boundaries.

4. Conclusions

Alumina-molybdenum composites sintered by selective laser sintering were proposed in this manuscript. Different molybdenum contents were studied: 0, 1, 2.5, 5, 10 and 20 wt %. It was possible to see that increasing the molybdenum content resulted in composites with less percentage of porosity. It is possible, for that reason, to say that increasing the molybdenum content results in greater densification rates, which could ensure the good characteristics of the alumina. The best results were observed in the case of the composite Al_2O_3-10 wt % Mo, with an average alumina grain size <10 µm and few pores. It is also observed for this molybdenum content that this element drastically affects the microstructural evolution during the sintering, mainly the final size of alumina, as this element, located at triple points and grain boundaries, inhibits the grain growth. On the other hand, results suggest that laser sintering could be an attractive method to sinter Al_2O_3–Mo ceramics in short times. This is particularly relevant when the molybdenum content is < 10 wt % Mo as greater contents involve the appearance of significant quantities of molybdenum (VI) oxide, which, apart from its potential volatilization and, thus losses of molybdenum, is

detrimental for the mechanical properties of the composite when it appears as inclusion.

Declaration of competing interest

The authors declare that they have no known competing financial interests or personal relationships that could have appeared to influence the work reported in this paper.

Acknowledgements

Daniel Fernández-González acknowledges the grant (Juan de la Cierva-Formación program) FJC2019-041139-I funded by MCIN/AEI/10.13039/501100011033 (Ministerio de Ciencia e Innovación, Agencia Estatal de Investigación).

We thank Dra. Nayely Pineda Aguilar for her support in the utilization of the Scanning Electron Microscope equipment.

Cristian Gómez-Rodríguez acknowledges the Universidad Veracruzana (Vicerrectoría Coatzacoalcos and Facultad de Ingeniería) for allowing him to make a short stay in the Nanomaterials and Nanotechnology Research Center (CINN-CSIC) and the University of Oviedo (Asturias, Spain) for research activities.

References

[1] J.S. Moya, S. López-Esteban, C. Pecharromán, The challenge of ceramic/metal microcomposites and nanocomposites, Prog. Mater. Sci. 52 (2000) 1017–1090, https://doi.org/10.1016/j.pmatsci.2006.09.003.

[2] P. Matteazzi, G. Le Caër, Synthesis of nanocrystalline alumina-metal composites by room-temperature ball-milling of metal oxides and aluminum, J. Am. Ceram. Soc. 75 (1992) 2749–2755, https://doi.org/10.1111/j.1151-2916.1992.tb05499.x.

[3] Y. Waku, M. Suzuki, Y. Oda, Y. Kohtoku, Improvement of fracture toughness of Al_2O_3 composites by micro-dispersion of flaky refractory metals Mo, Ta and Nb, J. Ceram. Soc. Jpn. 103 (1995) 713–719, https://doi.org/10.2109/jcersj.103.713.

[4] T. Sekino, T. Nakajima, S. Ueda, K. Niihara, Reduction and sintering of a nickel–dispersed-alumina composite and its properties, J. Am. Ceram. Soc. 80 (1997) 1139–1148, https://doi.org/10.1111/j.1151-2916.1997.tb02956.x.

[5] W.G. Fahrenholtz, D.T. Ellerby, R.E. Loehman, Al_2O_3–Ni composites with high strength and fracture toughness, J. Am. Ceram. Soc. 83 (2004) 1279–1280, https://doi.org/10.1111/j.1151-2916.2000.tb01368.x.

[6] E. Breval, G. Dodds, C.G. Pantano, Properties and microstructure of Ni-alumina composite materials prepared by the sol/gel method, Mater. Res. Bull. 20 (1985) 1191–1205, https://doi.org/10.1007/BF00542904.

[7] A. Miazga, K. Konopka, M. Gizowska, M. Szafran, Preparation of Al_2O_3–Ni cermet composites by aqueous gelcasting, Powder Metall. Met 52 (2014) 567–571, https://doi.org/10.1007/s11106-014-9561-y.

[8] T. Sekino, K. Niihara, Microstructural characteristics and mechanical properties for Al_2O_3/metal nanocomposites, Nanostruct. Mater. 6 (1995) 663–666, https://doi.org/10.1016/0965-9773(95)00145-X.

[9] W.-C.J. Wei, S.C. Wang, F.H. Cheng, Characterization of Al_2O_3 composites with fine Mo particulates, I Microstructural development, Acta Metall. 10 (1998) 965–981, https://doi.org/10.3390/ma14123398.

[10] L.A. Simpson, A. Wasylyshyn, Fracture energy of Al_2O_3 containing Mo fibers, J. Am. Ceram. Soc. 54 (1971) 56–57, https://doi.org/10.1111/j.1151-2916.1971.tb12171.x.

[11] D.T. Rankin, J.J. Stiglich, D.R. Petrak R. Ruh, Hot-pressing and mechanical properties of Al_2O_3 with a Mo-dispersed phase, J. Am. Ceram. Soc. 54 (1971) 277–281, https://doi.org/10.1111/j.1151-2916.1971.tb12290.x.

[12] N. Nawa, T. Sekino, K. Niihara, Fabrication and mechanical behaviour of Al_2O_3/Mo nanocomposites, J. Mater. Sci. 29 (1994) 3185–3192, https://doi.org/10.1007/BF00356661.

[13] S.-C. Wang, W.-C.J. Wei, Characterization of Al_2O_3 composites with Mo particulates, II. Densification and mechanical properties, Nanostruct. Mater. 10 (1998) 983–1000.

[14] P. Lada, A. Miazga, M. Zagorska, J. Zygmuntowicz, K. Konopka, Characterization of alumina–molybdenum composites prepared by gel casting method, Powder Metall. Met 58 (2019) 295–300, https://doi.org/10.1007/s11106-019-00073-0.

[15] K. Broniszewski, J. Wozniak, K. Czechowski, L. Jaworska, A. Olszyna, Al_2O_3–Mo cutting tools for machining hardened stainless steel, Wear 303 (2013) 87–91, https://doi.org/10.1016/j.wear.2013.03.002.

[16] J. Zygmuntowicz, A. Baczynska, A. Miazga, W. Kaszuwara, K. Konopka, Al_2O_3-Mo functionally graded material obtained via centrifugal slip casting, Ceram. Mater. 69 (2017) 73–77.

[17] Y.P. Kathuria, Microstructuring by selective laser sintering of metallic powder, Surf. Coating. Technol. 116–119 (1999) 643–649, https://doi.org/10.1016/S0257-8972(99)00266-2.

[18] P. Bertrand, F. Bayle, C. Combe, P. Goeuriot, I. Smurov, Ceramic components manufacturing by selective laser sintering, Appl. Surf. Sci. 254 (2007) 989–992, https://doi.org/10.1016/j.apsusc.2007.08.085.

[19] K. Wudy, L. Lanzl, D. Drummer, Selective laser sintering of filled polymer systems: bulk properties and laser beam material interaction, Phys. Procedia 83 (2016) 991–1002, https://doi.org/10.1016/j.phpro.2016.08.104.

[20] K. Murali, A.N. Chatterjee, P. Saha, R. Palai, S. Kumar, S.K. Roy, P.K. Mishra, A. R. Choudhury, Direct selective laser sintering of iron–graphite powder mixture, J. Mater. Process. Technol. 136 (2003) 179–185, https://doi.org/10.1016/S0924-0136(03)00150-X.

[21] L.V. García, M.I. Mendivil, T.K.D. Roy, G.A. Castillo, S. Shaji, Laser sintering of magnesia with nanoparticles of iron oxide and aluminum oxide, Appl. Surf. Sci. 336 (2015) 59–66, https://doi.org/10.1016/j.apsusc.2014.09.140.

[22] S.K. Ghosh, K. Bandyopadhyay, P. Saha, Development of an in-situ multi-component reinforced Al-based metal matrix composite by direct metal laser sintering technique — optimization of process parameters, Mater. Char. 93 (2014) 68–78, https://doi.org/10.1016/j.matchar.2014.03.021.

[23] W.N. Su, P. Erasenthiran, P.M. Dickens, Investigation of fully dense laser sintering of tool steel powder using a pulsed Nd: YAG (neodymium-doped yttrium aluminium garnet) laser, P. I. Mech. Eng. C- J. Mec. 217 (2003) 127–138, https://doi.org/10.1243/095440603762554677.

[24] E.O. Olakanmi, R.F. Cochrane, K.W. Dalgarno, Densification mechanism and microstructural evolution in selective laser sintering of Al–12Si powders, J. Mater. Process. Technol. 211 (2011) 113–121, https://doi.org/10.1016/j.jmatprotec.2010.09.003.

[25] B. Zhang, H. Liao, C. Coddet, Effects of processing parameters on properties of selective laser melting Mg–9%Al powder mixture, Mater. Des. 34 (2012) 753–758, https://doi.org/10.1016/j.matdes.2011.06.061.

[26] X. Su, Y. Yang, Research on track overlapping during selective laser melting of powders, J. Mater. Process. Technol. 212 (2012) 2074–2079, https://doi.org/10.1016/j.jmatprotec.2012.05.012.

[27] M. Agarwala, D. Bourell, J. Beaman, H. Marcus, J. Barlow, Direct selective laser sintering of metals, Rapid Prototyp. J. 1 (1995) 26–36, https://doi.org/10.1108/13552549510078113.

[28] E.O. Olakanmi, K.W. Dalgarno, R.F. Cochrane, Rapid Prototyp. J. 18 (2012) 109–119, https://doi.org/10.1108/13552541211212096.

[29] K. Subramanian, N. Vail, J. Barlow, H. Marcus, Selective laser sintering of alumina with polymer binders, Rapid Prototyp. J. 1 (1995) 24–35, https://doi.org/10.1108/13552549510086844.

[30] J. Deckers, J.-P. Kruth, K. Shahzad, J. Vleugels, Density improvement of alumina parts produced through selective laser sintering of alumina-polyamide composite powder, CIRP Annals 61 (2012) 211–214, https://doi.org/10.1016/j.cirp.2012.03.032.

[31] E.M. Fayed, A.S. Elmesalamy, M. Sobih, Y. Elshaer, Characterization of direct selective laser sintering of alumina, Int. J. Adv. Manuf. Technol. 94 (2018) 2333–2341, https://doi.org/10.1007/s00170-017-0981-y.

[32] I. Shishkovsky, I. Yadroitsev, Ph Bertrand, I. Smurov, Alumina–zirconium ceramics synthesis by selective laser sintering/melting, Appl. Surf. Sci. 254 (2007) 966–970, https://doi.org/10.1016/j.apsusc.2007.09.001.

[33] P.K. Subramanian, H.L. Marcus, Selective laser sintering of alumina using aluminum binder, Mater. Manuf. Process. 10 (1995) 689–706, https://doi.org/10.1080/10426919508935060.

[34] E.A. Gulbransen, K.F. Andrew, F.A. Brassart, Oxidation of molybdenum 550° to 1700°C, J. Electrochem. Soc. 110 (1963) 952, https://doi.org/10.1149/1.2425918.

[35] G. de Micco, H. Nassini, A.E. Bohé, Kinetics of molybdenum oxidation between 375 and 500°C, in: V.S. Saji, S.I. Lopatin (Eds.), Molybdenum and its Compounds: Applications, Electrochemical Properties and Geological Implication, Nova Publishers, New York, 2014, pp. 313–339.

[36] J. Guardia-Valenzuela, A. Bertarelli, F. Carra, N. Mariani, S. Bizzaro, R. Arenal, Development and properties of high thermal conductivity molybdenum carbide - graphite composites, Carbon 135 (2018) 72–84, https://doi.org/10.1016/j.carbon.2018.04.010.

[37] L.A. Diaz, A.F. Valdés, C. Díaz, A.M. Espino, R. Torrecillas, Alumina/molybdenum nanocomposites obtained in organic media, J. Eur. Ceram. Soc. 23 (2003) 2829–2834, https://doi.org/10.1016/S0955-2219(03)00295-4.

[38] A. Heidarpour, F. Karimzadeh, M.H. Enayati, Fabrication and characterisation of bulk Al_2O_3/Mo nanocomposite by mechanical milling and sintering, Powder Metall. 54 (2011) 513–517, https://doi.org/10.1179/003258910X12740974839585.

[39] D. Fernández-González, I. Ruiz-Bustinza, C. González-Gasca, J. Piñuela-Noval, J. Mochón-Castaños, J. Sancho-Gorostiaga, L.F. Verdeja, Concentrated solar energy applications in materials science and metallurgy, Sol. Energy 170 (2018) 520–540, https://doi.org/10.1016/j.solener.2018.05.065.

[40] G. Flamant, A. Ferriere, D. Laplaze, C. Monty, Solar processing of materials: opportunities and new frontiers, Sol. Energy 66 (1999) 117–132, https://doi.org/10.1016/S0038-092X(98)00112-1.

[41] D. Fernández-González, J. Prazuch, I. Ruiz-Bustinza, C. González-Gasca, J. Piñuela-Noval, L.F. Verdeja, Iron metallurgy via concentrated solar energy, Metals 8 (2018) 873, https://doi.org/10.3390/met8110873.

[42] D. Fernández-González, J. Prazuch, I. Ruiz-Bustinza, C. González-Gasca, J. Piñuela-Noval, L.F. Verdeja, Solar synthesis of calcium aluminates, Sol. Energy 171 (2018) 658–666, https://doi.org/10.1016/j.solener.2018.07.012.

[43] D. Fernández-González, J. Prazuch, I. Ruiz-Bustinza, C. González-Gasca, J. Piñuela-Noval, L.F. Verdeja, Transformations in the Mn-O-Si system using concentrated

solar energy, Sol. Energy 184 (2019) 148–152, https://doi.org/10.1016/j.solener.2019.04.004.
[44] D. Fernández-González, J. Prazuch, I. Ruiz-Bustinza, C. González-Gasca, J. Piñuela-Noval, L.F. Verdeja, Transformations in the Si-O-Ca system: silicon-calcium via solar energy, Sol. Energy 181 (2019) 414–423, https://doi.org/10.1016/j.solener.2019.02.026.
[45] D. Fernández-González, J. Prazuch, I. Ruiz-Bustinza, C. González-Gasca, J. Piñuela-Noval, L.F. Verdeja, The treatment of Basic Oxygen Furnace (BOF) slag with concentrated solar energy, Sol. Energy 180 (2019) 372–382, https://doi.org/10.1016/j.solener.2019.01.055.
[46] D. Fernández-González, J. Prazuch, I. Ruiz-Bustinza, C. González-Gasca, C. Gómez-Rodríguez, L.F. Verdeja, Recovery of copper and magnetite from copper slag using concentrated solar power (CSP), Metals 11 (2022) 1032, https://doi.org/10.3390/met11071032.
[47] M. Suárez, D. Fernández-González, L.A. Díaz, A. Borrell, J.S. Moya, A. Fernández, Synthesis and processing of improved graphite-molybdenum-titanium composites by coloidal route and spark plasma sintering, Ceram. Int. 47 (2021) 30993–30998, https://doi.org/10.1016/j.ceramint.2021.07.267.
[48] M. Suárez, D. Fernández-González, C.F. Gutiérrez-González, L.A. Díaz, A. Borrell, J. S. Moya, R. Torrecillas, A. Fernández, Effect of green body density on the properties of graphite-molybdenum-titanium composite sintered by spark plasma sintering, J. Eur. Ceram. Soc. 42 (2022) 2048–2054, https://doi.org/10.1016/j.jeurceramsoc.2021.12.073.
[49] S.J.J. Kumar, Selective laser sintering: a qualitative and objective approach, JOM-J. Min. Met. Mat. S. 55 (2003) 43–47, https://doi.org/10.1007/s11837-003-0175-y.
[50] J.P. Kruth, X. Wang, T. Laoui, L. Froyen, Lasers and materials in selective laser sintering, Assemb. Autom. 23 (2003) 357–371, https://doi.org/10.1108/01445150310698652.
[51] E.M. Mohamed, S.F. Barakh Ali, Z. Rahman, S. Dharani, T. Ozkan, M. A. Kuttolamadom, M.A. Khan, Formulation optimization of selective laser sintering 3D-Printed tablets of clindamycin palmitate hydrochloride by response surface methodology, AAPS PharmSciTech 21 (2020) 232, https://doi.org/10.1208/s12249-020-01775-0.
[52] Y.A. Gueche, N.M. Sanchez-Ballester, S. Cailleaux, B. Bataille, I. Soulairol, Selective laser sintering (SLS), a new chapter in the production of solid oral forms (SOFs) by 3D printing, Pharmaceutics 13 (2021) 1212, https://doi.org/10.3390/pharmaceutics13081212.
[53] P. Muthuswamy, Additive manufacturing of tungsten carbide hardmetal parts by selective laser melting (SLM), selective laser sintering (SLS) and binder jet 3D printing (BJ3DP) techniques, Lasers Manuf. Mater. Process. 7 (2020) 338–371, https://doi.org/10.1007/s40516-020-00124-0.
[54] F. Fina, A. Goyanes, S. Gaisford, A.W. Basit, Selective laser sintering (SLS) 3D printing of medicines, Int. J. Pharm. (Amst.) 529 (2017) 285–293, https://doi.org/10.1016/j.ijpharm.2017.06.082.
[55] E. Balliu, H. Andersson, M. Engholm, T. Öhlund, H.-E. Nilsson, H. Olin, Selective laser sintering of inkjet-printed silver nanoparticle inks on paper substrates to achieve highly conductive patterns, Sci. Rep. 8 (2018), 10408, https://doi.org/10.1038/s41598-018-28684-4.
[56] A. Franco, M. Lanzetta, L. Romoli, Experimental analysis of selective laser sintering of polyamide powders: an energy perspective, J. Clean. Prod. 18 (2010) 1722–1730, https://doi.org/10.1016/j.jclepro.2010.07.018.
[57] J.P. Kruth, M.C. Leu, T. Nakagawa, Progress in additive manufacturing and rapid prototyping, CIRP Annals 47 (1998) 525–540, https://doi.org/10.1016/S0007-8506(07)63240-5.